V. W. Antonetti
Manager,
Advanced Thermal Laboratory,
International Business Machines Corporation,
Data Systems Division,
Poughkeepsie, N.Y.
Mem. ASME

M. M. Yovanovich
Professor,
Department of Mechanical Engineering,
Thermal Engineering Group,
University of Waterloo,
Ontario, Canada
Mem. ASME

Enhancement of Thermal Contact Conductance by Metallic Coatings: Theory and Experiment

A thermomechanical model for nominally flat, rough contacting surfaces coated with a metallic layer is developed. The model is shown to agree quite well with thermal test data obtained using nickel specimens, with one side of the contact coated with silver and the other side glass-bead blasted. In addition, it is demonstrated that a coated joint can be reduced to an equivalent bare joint by employing an effective hardness and an effective thermal conductivity. Using this technique, 61 coated test points were correlated, with an RMS difference of ±12.6 percent between the data and a correlation which had previously been used only for bare contacts.

Introduction

The success of a thermal design often requires that the heat transfer coefficient across an interface be enhanced, that is, improved over the bare joint situation. Techniques commonly employed include the application of a thermal grease to the contacting surfaces [1, 2], insertion of a soft metal foil at the interface [3, 4], and coating one or both of the contacting surfaces with a relatively soft metal [2, 5, 6].

Metallic coatings are an important enhancement alternative because a user can avoid the handling problem often associated with soft foils, and the contamination problem which often makes chemically active thermal greases objectionable. Despite the importance of metallic coatings, however, the only attempt to develop an overall thermomechanical model is by O'Callaghan et al. [5]. They also conducted experiments on abutting stainless steel specimens, where one side of the interface was coated with tin. Because their test apparatus was severely underpowered, the reported interface temperature differences were extremely small, casting doubt on the reliability of the data. Furthermore, the model of O'Callaghan et al. does not predict their own data very well.

A solution for only the *thermal portion* of a coated contact, albeit with different boundary conditions, has been described in [7, 8]. The constriction resistance was determined for a finite cylindrical flux tube with a hot spot located on a layer and a Robin condition specified at the end opposite the contact. However, the complications introduced by the boundary condition of the third kind are not required in the present application, and therefore, the thermal problem remains to be solved using more appropriate boundary conditions.

With regard to the *mechanical portion*, thermal contact resistance correlations for bare surfaces, for example [9], require as input the microhardness of the softer material. It is reasonable to assume in enhancement situations that the softer of the two contacting surfaces will be the metallic layer. Clearly, when the layer is very thick the microhardness to employ would be that of the layer. As the layer thickness decreases it is equally clear that the microhardness will increase, approaching the microhardness of the substrate as the layer thickness approaches zero. But what of the intermediate condition? Although analytical studies have been done regarding elastic contact stress in layers [10], no relevant analysis could be found relating to the equivalent plastic situation.

The purpose of the present work, therefore, is to develop a thermomechanical model for the prediction of the contact conductance of nominally flat, rough surfaces enhanced with a metallic coating, and to verify the theory by experiment.

Theoretical Analysis

Before beginning, it is appropriate to state the assumptions inherent in the analysis that will follow:

1 Contacting surfaces are clean, free of oxides, etc., and contact occurs in a vacuum. Radiation across the interface and conduction across the interstitial gaps are negligible.

2 Contacting surfaces are microscopically rough but macroscopically flat and have a Gaussian height distribution.

3 In general, the real pressure between contacting surfaces is equal to the microhardness of the softer material. When either of the contacting surfaces is coated with a soft metal, the real pressure between the surfaces is equal to the "effective microhardness" of the layer-substrate combination. (More will be said of this later.)

4 The real contact area consists of circular, isothermal, microcontact spots which are distributed uniformly over the apparent area. When a layer is present, the contact is also assumed to be a circular spot, but now residing on the top of the layer. In other words, penetration of the harder surface into the layer, which undoubtedly occurs to some extent, is ignored to simplify the subsequent thermal analysis. This is at least partially justifiable on the basis of [11] wherein solutions were obtained for the constriction resistance of numerous symmetric and nonsymmetric, singly connected, planar geometries. The conclusion of the latter study was that the constriction resistance of an arbitrary contact was approximately equal to a circular contact of equal area. It is assumed that this conclusion would also apply to arbitrary contact shapes on a layer.

5 The contact between the layer and the substrate is "perfect." It has been shown [12] that the resistance of a so-called perfect joint is about two orders of magnitude less than the constriction resistance expected here.

6 When a surface is coated, the surface characteristics are the same as the underlying substrate [6].

Uncoated Contacting Surfaces. Clearly the development of a predictive model for coated contacts will be based, in large measure, on what is known about bare contacts. With the assumptions already made, the heat transfer across a bare joint will be confined to the discrete microcontacts formed by the contacting asperities. If a total of N circular microcontacts, having a mean radius a, are distributed over the apparent contact area, we can write the joint resistance as [9]

Contributed by the Heat Transfer Division for publication in the JOURNAL OF HEAT TRANSFER. Manuscript recevied by the Heat Transfer Division March 1, 1984.

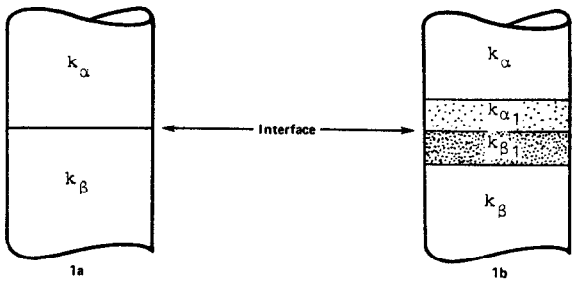

Fig. 1 Contact of bare and coated joint

$$R_j = \frac{1}{N}\left[\frac{\psi(\epsilon)}{4k_\alpha a} + \frac{\psi(\epsilon)}{4k_\beta a}\right] \tag{1}$$

where k_α and k_β are the thermal conductivities of the contacting surfaces shown in Fig. 1(*a*).

The constriction parameter $\psi(\epsilon)$ has been evaluated by several authors [13-16]. In [17] it was shown that the constriction parameter can also be approximated by the following power law correlation

$$\psi(\epsilon) = 0.76\left(\frac{P}{H}\right)^{-0.027} \tag{2}$$

where the error is ±1 percent in the range $10^{-4} \le P/H \le 10^{-2}$. An expression for the mean contact spot radius was derived in [16], which, as shown in [17], can be approximated using the following power law correlation

$$a = 0.77\left(\frac{\sigma}{m}\right)\left(\frac{P}{H}\right)^{0.097} \tag{3}$$

where the error is ±4.5 percent in the range $10^{-4} \le P/H \le 10^{-2}$. A simple force balance at the contacting surface can be used to determine the total number of microcontacts per unit area as

$$\frac{N}{A_a} = \frac{1}{\pi a^2}\left(\frac{P}{H}\right) \tag{4}$$

By substituting equation (4) into equation (1), and noting that the resistance is the reciprocal of the product of the joint conductance and the apparent contact area, the general expression for the thermal conductance across a bare interface becomes

$$\frac{1}{h_j} = \frac{\pi a}{4}\left(\frac{H}{P}\right)\left[\frac{\psi(\epsilon)}{k_\alpha} + \frac{\psi(\epsilon)}{k_\beta}\right] \tag{5}$$

Coated Contacting Surfaces. When a joint is coated, the effective microhardness H' of the layer-substrate combination will, of course, be different from that of a bare joint. This results in a change in the total number of microcontact spots needed to support the load, in a different contact spot radius a', and a different constriction parameter $\psi(\epsilon', \phi_n)$. In this case, the constriction parameter not only depends upon the relative mean contact spot size ϵ', but also upon a modification factor ϕ_n, which is some function of the relative layer thickness τ and substrate-to-layer thermal conductivity ratio K.

By referring to Fig. 1(*b*), an expression for the thermal contact conductance across a joint with a layer on both sides of the contact can be obtained by rewriting equation (5) as

$$\frac{1}{h_j'} = \frac{\pi a'}{4}\left(\frac{H'}{P}\right)\left[\frac{\psi(\epsilon', \phi_{n_\alpha})}{k_\alpha} + \frac{\psi(\epsilon', \phi_{n_\beta})}{k_\beta}\right] \tag{6}$$

Equation (6) can be cast in a more convenient form by introducing a constriction parameter correction factor defined as the ratio of the constriction parameter with a layer to that without a layer, for the same value of the relative contact radius, that is $C = \psi(\epsilon', \phi_n)/\psi(\epsilon')$. Then equation (6) becomes

$$\frac{1}{h_j'} = \frac{\pi a'}{4}\left(\frac{H'}{P}\right)\psi(\epsilon')\left[\frac{C_\alpha}{k_\alpha} + \frac{C_\beta}{k_\beta}\right] \tag{7}$$

Using the approximation for the constriction parameter given by equation (2), and the approximate expression for the contact spot radius equation (3), we obtain the following ratios:

$$\frac{\psi(\epsilon)}{\psi(\epsilon')} = \left(\frac{H}{H'}\right)^{0.027} \tag{8}$$

and

$$\frac{a}{a'} = \left(\frac{H'}{H}\right)^{0.097} \tag{9}$$

Now, we divide equation (5) by equation (7), and substitute into the resulting expression equations (8) and (9). After rearrangement this yields

$$h_j' = h_j\left(\frac{H}{H'}\right)^{0.93}\left[\frac{k_\alpha + k_\beta}{C_\alpha k_\beta + C_\beta k_\alpha}\right] \tag{10}$$

Inspection of equation (10) reveals that the contact conductance of a joint with a layer on both sides of an interface is equal to the bare joint conductance multiplied by two terms: The first term will be defined as a mechanical augmentation factor, and the second as a thermal augmentation factor.

Coated Contacting Surfaces (Alternate Analyis). Referring again to Fig. 1(*b*), we can also obtain the thermal contact resistance for a joint when a layer is presented by rewriting equation (1), with the primed quantities being associated with

Nomenclature

a = contact spot radius
A = area
b = flux tube radius
C = constriction parameter correction factor
d = equivalent Vickers indentation depth
H = Vickers microhardness
H' = effective microhardness of soft layer on harder substrate
h = thermal contact conductance
J_n = Bessel function, first kind, order n
K = thermal conductivity ratio (substrate to layer)
k = thermal conductivity
k' = effective thermal conductivity
m = combined average absolute asperity slope = $\sqrt{m_\alpha^2 + m_\beta^2}$
N = number of contact spots in apparent area A_a
P = apparent contact pressure
R = thermal resistance
t = layer thickness
γ_n = constriction parameter modification factor attributable to contact temperature basis
λ_n = eigenvalues
ϵ = relative mean contact spot radius = $a/b = \sqrt{P/H}$
δ_n = roots of $J_1(\delta_n) = 0$
ρ_n = constriction parameter modification factor attributable to heat flux distribution
σ = combined RMS roughness = $\sqrt{\sigma_\alpha^2 + \sigma_\beta^2}$
τ = relative layer thickness = (t/a)
ϕ_n = constriction parameter modification factor attributable to the layer
$\psi(\epsilon)$ = constriction parameter

Superscripts

$'$ = layer

Subscripts

a = apparent
c = contact or constriction
j = joint
L = layer
s = substrate
v = Vickers
α = one side of contact
β = other side of contact

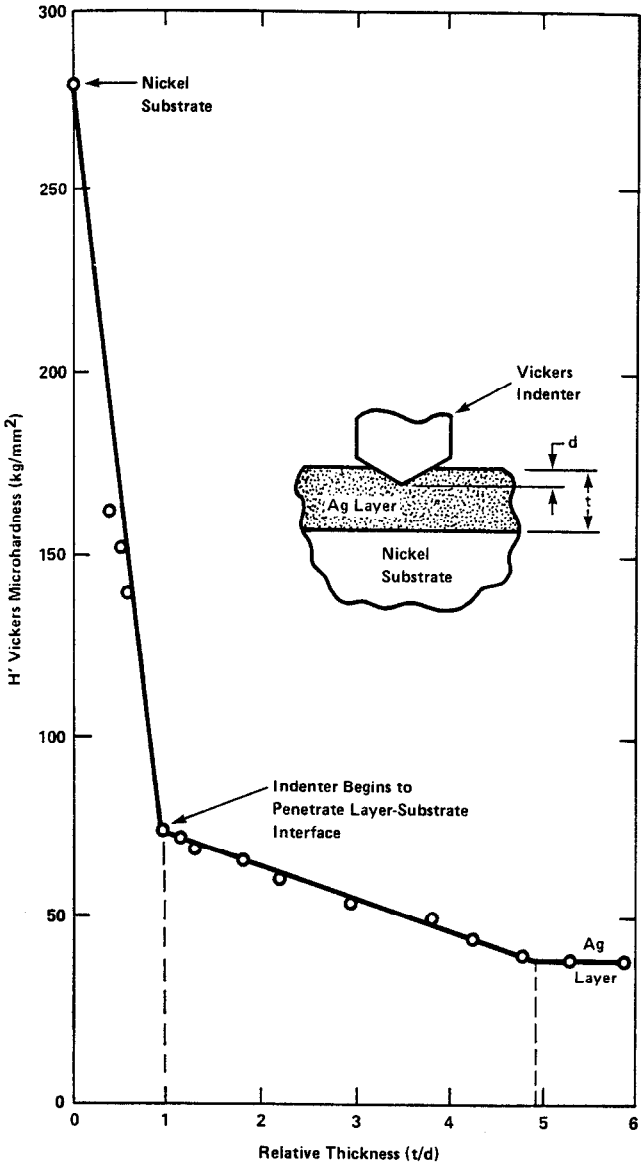

Fig. 2 Vickers microhardness of silver layer on nickel substrate

the layers. When the definition of the constriction parameter correction factor is accounted for, the result is

$$R_j' = \frac{\psi(\epsilon')}{4N'a'}\left[\frac{C_\alpha}{k_\alpha} + \frac{C_\beta}{k_\beta}\right] \tag{11}$$

Now an effective thermal conductivity is defined as

$$k' = \frac{2k_\alpha k_\beta}{C_\alpha k_\beta + C_\beta k_\alpha} \tag{12}$$

Then the contact resistance for a coated joint reduces to

$$R_j' = \frac{\psi(\epsilon')}{2a'N'k'} \tag{13}$$

where a' is given by equation (3) and N' by equation (4). Note that both quantities depend on the effective microhardness H'.

Equation (13) yields numerical results identical to equation (10), but has the same algebraic form as the equivalent expression for the contact resistance of a bare joint. This has the advantage of allowing a direct numerical comparison of the parameters that contribute to the contact resistance for both the bare and coated cases.

Regardless of which of the two previous analytical approaches is used, in order to determine the theoretical contact conductance for a coated joint, the effective microhardness of the particular layer-substrate combination being considered must be evaluated by mechanical analysis or by experimental means, and a thermal analysis must be performed to determine the constriction parameter correction factor due to the layer.

Thermal Analysis of a Coated Contact. The thermal portion of the analysis requires the solution of Laplace's equation for heat flow from a single concentric circular hot spot residing on a layer at the end of an infinite right circular cylinder whose walls are adiabatic. The complete solution is presented in [17]. In summary, the constriction parameter (for example on the α side) is first defined as

$$\psi(\epsilon', \phi_n) = 4k_\alpha a' R_c' \tag{14}$$

Then, after determining the constriction resistanace R_c', using an approach similar to [7, 8], the constriction parameter for a coated contact is shown to be

$$\psi(\epsilon', \phi_n) = \frac{16}{\pi\epsilon'}\sum_{n=1}^{\infty}\frac{J_1^2(\delta_n'\epsilon')}{(\delta_n')^3 J_0^2(\delta_n')}\phi_n \cdot \gamma_n \cdot \rho_n \tag{15}$$

Equation (15) is nothing more than the expression for the dimensionless constriction parameter for a bare contact, with a uniform heat flux at the contact and the resistance based on the average contact temperature, as derived in [15], multiplied by three modification factors.

The first modification factor ϕ_n accounts for the influence of the layer; the second γ_n accounts for the contact temperature basis used in determining the constriction resistance (average, isothermal or centroidal); and the third ρ_n accounts for the contact heat flux distribution assumed.

For abutting surfaces, it is usual to assume that the contact spots are isothermal. The modification factors in this case are $\gamma_n = 1$, and

$$\phi_n = K\left[\frac{(1+K)+(1-K)\exp(-2\delta_n'\epsilon'\tau')}{(1+K)-(1-K)\exp(-2\delta_n'\epsilon'\tau')}\right] \tag{16}$$

and

$$\rho_n = \frac{\sin(\delta_n'\epsilon')}{2J_1(\delta_n'\epsilon')} \tag{17}$$

The constriction parameter correction factor is now obtained by dividing the constriction parameter with a layer present, that is equation (15), by an expression for the constriction parameter without a layer, that is equation (15) with $\phi_n = 1$. The reader is referred to [17] for a tabulation of numerical values.

Mechanical Analysis of a Coated Joint. In the following discussion, a methodology is outlined which allows the determination of the effective microhardness H' of a soft metallic layer on a harder substrate. The approach is semiempirical.

Vickers Microhardness Distribution. Figure 2 shows the results of Vickers microhardness measurements performed on Nickel 200 specimens with differing vapor-deposited silver coating thickness. (This is the layer-substrate combination used in the thermal tests described in the next section.) Several other layer-substrate combinations were tested as well, and all exhibited similar characteristic curves. The results are contained in [17].

The open literature reveals no similar research in this area. The search for a physical explanation of observed results leads to the work of Mulhearn [18]. By plotting equal strain contours under indenters, Mulhearn showed that material is displaced radially outward from the indentation. This suggests the following interpretation of the microhardness data from the present study. By referring to Fig. 2, it can be seen that in the region $t/d > 4.9$, the effective microhardness equals the layer microhardness. In this case, the indenter and the elastic-plastic boundary are wholly within the layer. In the intermediate region $1.0 \leq t/d \leq 4.9$, the indenter is still

totally within the layer but the elastic-plastic boundary has expanded to the point where it is distorted by the underlying harder substrate, and because of this the effective microhardness gradually increases. At $t/d = 1.0$, the indenter has penetrated the layer and is influenced directly by the underlying substrate. As a consequence, the slope of the curve changes abruptly and the effective microhardness increases until it reaches the substrate microhardness value at $t/d = 0$.

Effective Microhardness. Rather than a single indenter, let us now consider a multiplicity of indenters, as when a hard, rough surface is put in contact with a softer layer. What is proposed here is that the effective microhardness for this situation can be determined from a Vickers microhardness curve appropriate for the materials combination, such as for silver on nickel, as shown in Fig. 2. With this assumption, the following effective microhardness equations are obtained from Fig. 2. In the region $t/d < 1.0$

$$H' = H_s\left(1 - \frac{t}{d}\right) + 1.81\, H_L\left(\frac{t}{d}\right) \tag{18}$$

and in the region $1.0 \le t/d \le 4.9$

$$H' = 1.81\, H_L - 0.208\, H_L\left(\frac{t}{d} - 1\right) \tag{19}$$

When $t/d > 4.90$ the effective microhardness equals the layer microhardness.

In equations (18) and (19), d is the equivalent Vickers indentation depth of the harder contacting surface. In order to determine d, it is necessary to understand how a Vickers indentation is determined from microhardness measurements.

When a Vickers indenter is pressed into a surface it leaves a square indentation. By geometry the indentation depth is equal to the measured half-diagonal a_v multiplied by the slope of the Vickers indenter m_v, i.e., $d = m_v a_v$. But the asperities of an actual indenting hard, rough surface have an average asperity radius a and an average slope m. So in order to use Fig. 2 the average asperity indentation depth must be adjusted to an equivalent Vickers depth. This is accomplished by first setting the cross-sectional area of the contacting asperity equal to the projected area of a Vickers indentation; that is $a_v = a\sqrt{\pi/2}$. Now, combining the simple relationships immediately preceding, and substituting equation (3) for the asperity contact radius yields

$$d = 0.77\sqrt{\frac{\pi}{2}}\left(\frac{m_v}{m}\right)\sigma\left(\frac{P}{H'}\right)^{0.097} \tag{20}$$

Next, one has a choice of letting the asperity slope m in equation (20) remain a variable, or of fixing it at the Vickers value of 0.286. (The asperity slopes for the experimental portion of this work ranged from 0.129 to 0.350.) The thermomechanical model was compared to experimental data using both alternatives. Since neither of the alternatives consistently predicted the data better than the other, it was decided to fix the slope at the Vickers value because this minimized the overall RMS difference between the model and the data. This is equivalent to assuming, in equation (20), that $m_v/m = 1.0$. Implicit in this assumption is that Vickers indenters with slopes in the range cited will produce an effective microhardness curve identical to Fig. 2. With this assumption, equation (20) becomes

$$d = 0.97\,\sigma\left(\frac{P}{H'}\right)^{0.097} \tag{21}$$

It is interesting to note that the indentation depth is primarily dependent on the RMS roughness of the indenting surface and is a weak function of P/H'. In addition, because the indentation depth depends upon the effective microhardness, and the depth must be known to determine the effective microhardness, an iterative approach is required. Convergence is very rapid, however, because the indentation depth is such a weak function of the effective microhardness.

Table 1 Test specimen characteristics

Series	Specimens	Bare σ	Bare m	Coated σ	Coated m	t
A	08/09	4.29	0.239	0.16	0.025	0.0
	10/11	4.27	0.236	0.17	0.024	0.0
	12/13	4.06	0.231	0.19	0.030	1.4
	14/15	4.24	0.233	0.20	0.031	5.1
	16/17	4.45	0.252	0.27	0.038	39.5
	18/19	4.38	0.232	0.14	0.022	0.81
	22/23	4.19	0.224	0.21	0.027	1.2
	Average	4.26	0.234	0.19	0.028	
	Series A combined values: $\sigma = 4.27$, $m = 0.236$					
B	24/25	1.24	0.129	0.17	0.025	1.2
	26/27	1.21	0.137	0.19	0.024	0.0
	36/37	1.30	0.140	0.14	0.018	6.3
	Average	1.27	0.135	0.155	0.022	
	Series B combined values: $\sigma = 1.28$, $m = 0.137$					
C	28/29	8.62	0.350	0.14	0.018	2.4
	30/31	8.31	0.338	0.17	0.025	7.2
	32/33	8.03	0.348	0.19	0.024	18.0
	34/35	8.48	0.344	0.14	0.018	0.0
	Average	8.32	0.345	0.17	0.022	
	Series C combined values: $\sigma = 8.32$, $m = 0.346$					

Specimen material: Nickel 200
Cross-sectional area: 0.000641 m^2
σ = RMS roughness, μm
m = average absolute asperity slope, radians
t = coating thickness, μm

Averages consider only coated specimen pairs.
Combined values are for an equivalent rough surface against a perfect smooth.

Regarding the substrate microhardness H_S in equation (18) it should be noted that manufacturing processes such as lapping produce a surface microhardness layer. In these cases, it has been demonstrated [19, 20] that the use of the bulk microhardness for predicting contact conductance is incorrect. Instead, the method outlined in [19, 20] should be used to determine an appropriate microhardness value for the substrate.

Application of Theoretical Model. The reader is referred to [21] where the utility of the model developed here is illustrated by using it to analyze a common electronics packaging problem: heat transfer across a coated aluminum joint.

Experimental Program

Coated contact resistance test data in the open literature were found to be either unreliable [5], or to have inadequate test specimen surface characterization [2, 6]. An experimental program was undertaken, therefore, in order to generate test data against which to compare the theoretical model.

Specimens, Properties, and Test Parameters. Test specimens, fabricated from a single Nickel 200 rod, were finished to 28.6 mm diameter by 31.8 mm long, with both ends lapped smooth to a flatness deviation less than 1 μm. The specimens were tested in pairs, with one of the pair treated further by glass-bead blasting one end to a specified roughness. The other specimen was either left bare or had a layer of silver vapor deposited on one end. The characteristics of the test specimens are shown in Table 1. As shown in Table 1, three groups of test specimens were tested. The first, designated Series A, had a combined (or equivalent) surface roughness of 4.27 μm. Series B had a combined roughness of 1.28 μm, and the final group, Series C, had a combined roughness of 8.32 μm.

Details of the contact resistance test apparatus and the test procedure have been fully described elsewhere [17, 20]. In brief, contact resistance measurements were made in a vacuum chamber. The direction of heat flow was from the

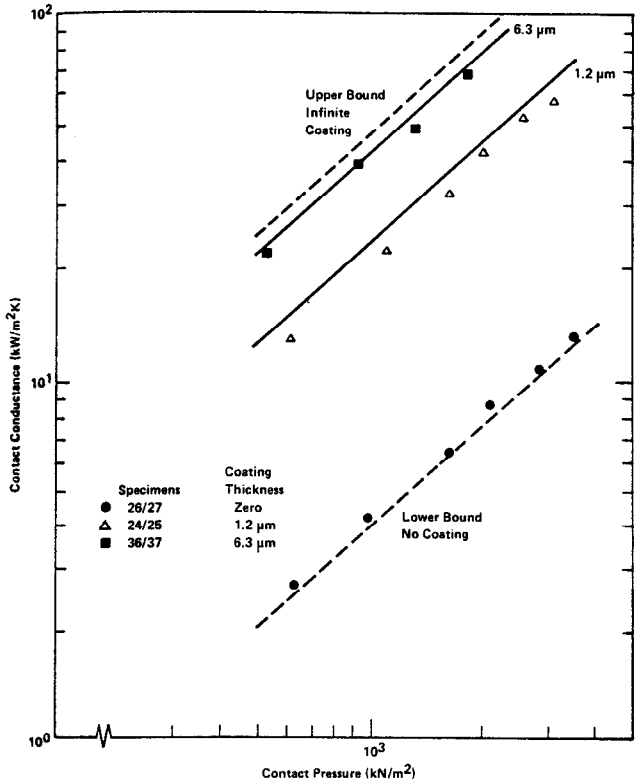

Fig. 3 Test results: contact conductance versus pressure (σ = 1.28 μm)

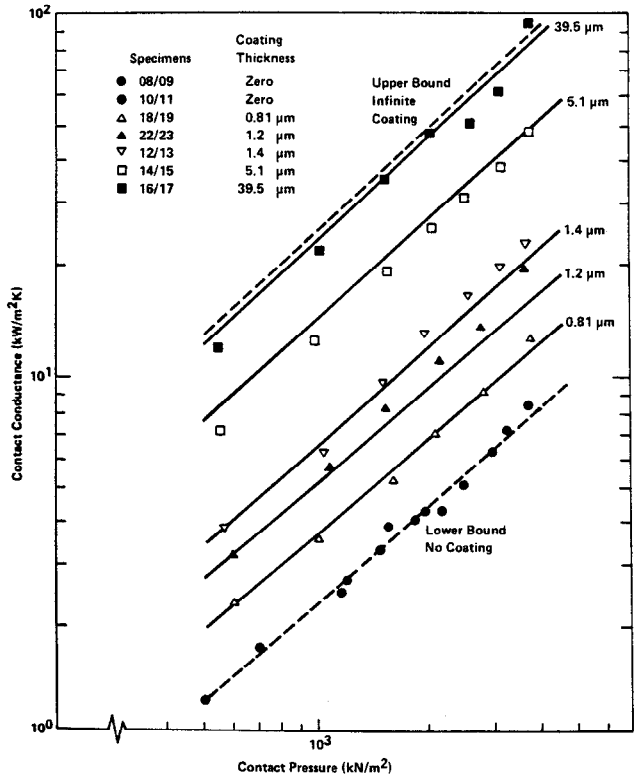

Fig. 4 Test results: contact conductance versus pressure (σ = 4.27 μm)

bare, glass-bead-blasted upper specimen to the silver-coated lower specimen. The range of the experimental parameters was approximately as follows: The heat flux varied from 2000 to 7000 kW/m^2; the contact pressure from 500 to 3700 kN/m^2; the interfacial temperature differences from 1.7 to 50°C (it should be noted that the majority of the temperature differences were greater than 10°C); and the mean interface

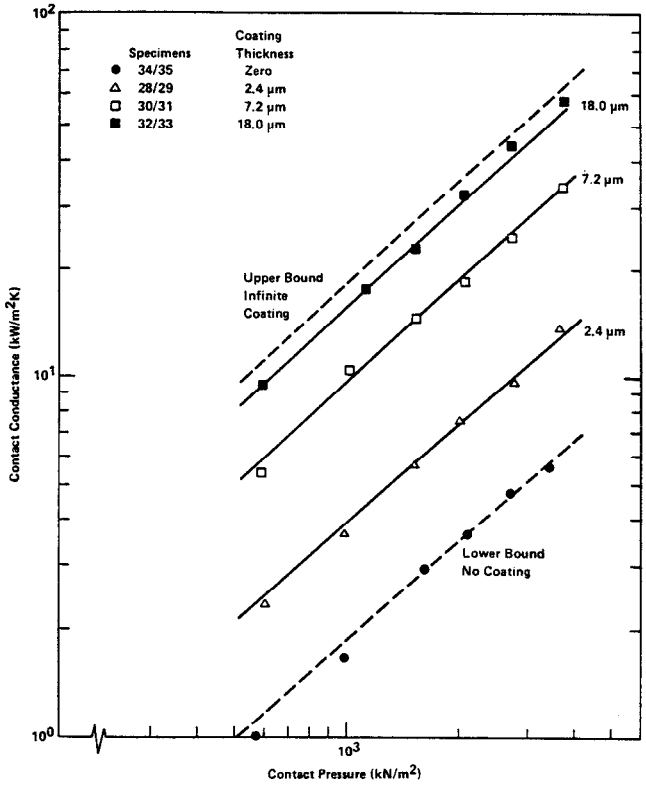

Fig. 5 Test results: contact conductance versus pressure (σ = 8.32 μm)

temperature varied from 85 to 206°C. The experimental error in the test setup was estimated to be ±4.5 percent.

Initially, thermal tests were conducted on the bare specimens, which can be considered the zero layer thickness case, or in other words the lower bound on the coated contact conductance. The test results for the bare joints have been previously reported in [21]. In summary, the agreement between the bare joint test data and Yovanovich's correlation [9] was excellent, with the RMS difference being only ±5.6 percent, provided the appropriate effective surface microhardness for the lapped surface is employed in the relative load expression.

Comparison of Coated Specimen Data Versus Model. For the coated test specimens, test results are compared to the proposed thermomechanical model, given by equation (10), in Figs. 3–5. It should be noted that the line representing the predicted performance for each specimen pair was computed using thermophysical properties determined as follows: First, contact temperatures for a given upper and lower specimen pair were determined at each test point. Next, average contact temperatures were calculated using the test data for all the runs experienced by the specimen pair. Then, based on these average contact temperatures, the thermal conductivity for the nickel substrates of the upper and lower specimens and for the silver layer were determined. The effective microhardness, on the other hand, was based on room temperature Vickers microhardness measurements. This is justified by test data [17, 22] which indicated that significant softening of the silver layer did not occur at the contact temperature levels in the present experiment.

The RMS difference between the theoretical model and the experimental results is as follows: Series A: ±11.3 percent, Series B: ±7.5 percent, and Series C: ±6.9 percent.

Figure 3 presents a plot of the contact conductance versus test pressure for Series B experiments, that is for the set of specimens with a combined surface roughness of 1.28 μm. As can be seen from Fig. 3, the coated contact conductance is

Table 2 Summary of calculated theoretical parameters and contact resistances for specimens at test pressure of approximately 2000 kN/m²

	P	t	t/d	H'	$\psi(\epsilon')$	C	k'	a'	N'	R'
Series B: Average Roughness = 1.28 μm										
26/27	2105	0.0	0.0	360.0	0.9636	1.000	64.5	3.3	11200	0.2025
24/25	2032	1.2	1.77	65.9	0.9171	0.428	87.7	4.2	36500	0.0342
36/37	1817	6.3	9.40	40.0	0.8996	0.198	103.9	4.3	52900	0.0194
Series A: Average roughness = 4.27 μm										
08/09	1925	0.0	0.0	300.0	0.9619	1.000	67.2	6.8	2930	0.3619
18/19	2055	0.8	0.38	214.0	0.9534	0.644	80.5	7.4	3660	0.2189
22/23	2107	1.2	0.57	169.9	0.9471	0.565	84.0	7.5	4600	0.1636
12/13	1922	1.4	0.68	144.2	0.9452	0.518	84.7	7.1	5530	0.1424
14/15	2005	5.1	2.19	62.4	0.9154	0.291	97.4	8.0	10500	0.0561
16/17	1990	39.5	17.10	40.0	0.8951	0.159	107.2	8.1	15900	0.0325
Series C: Average roughness = 8.32 μm										
34/35	2080	0.0	0.0	280.0	0.9590	1.000	67.1	9.4	1730	0.4364
28/29	1990	2.4	0.55	164.8	0.9478	0.480	86.9	9.9	2540	0.2145
30/31	2023	7.2	1.58	67.5	0.9182	0.287	97.7	10.8	5380	0.0811
32/33	2027	18.0	3.96	47.8	0.9030	0.190	105.1	10.5	8070	0.0509

Note: P = pressure, kN/m²
t = layer thickness, μm
t/d = dimensionless indentation depth
H' = effective hardness, kg/mm²
$\psi(\epsilon')$ = constriction parameter
C = constriction parameter correction factor
k' = effective thermal conductivity, W/m K
a' = contact spot radius, μm
N' = total number of microcontacts
R' = theoretical contact resistance, K/W

bounded by the bare joint, or zero layer thickness line (the lower bound), and by the infinitely thick silver layer case (the upper bound). There is approximately one order of magnitude between the two bounds.

Figure 4 is for Series A experiments, that is for the set of specimens with a combined surface roughness of 4.27 μm. In this case, a 1.2-μm layer thickness is seen to improve the contact conductance to a much lesser degree than for the comparable layer thickness in Fig. 3. Indeed, the relative enhancement effect for all the specimens tested in this series is not as pronounced as for those tested against the smoother surfaces in Fig. 3.

As can be seen in Fig. 5 (Series C: 8.32 μm combined roughness), the general tendency is the same, that is for a given layer thickness the relative improvement is less than is observed for the smoother 1.28 and 4.27-μm cases. This is attributed to the fact that a rough surface penetrates the layer more deeply than would a smoother contacting surface, and hence is more affected by the harder substrate under the layer, which results in a higher effective microhardness and, in turn, a lower contact conductance. This leads to the general conclusion that a given layer thickness will have more of an enhancement effect as the roughness of the bare contacting surface is decreased.

It is interesting to examine the parameters involved in the calculation of the theoretical contact resistance for all the specimens tested. Table 2 summarizes the results of such a calculation. Since all the computations were performed at the same approximate test pressure, the test specimen pairs differ only in the texture of the bare contacting surface and in the thickness of the metallic layer. From the table, it is seen that the effective microhardness H' diminishes quite rapidly as the layer thickness increases. As expected, for a given layer thickness, the lowest effective microhardness value occurs when the layer is in contact with the smoothest abutting surface. Table 2 also shows that the contact spot radius a' is determined primarily by the surface texture and influenced in only a minor way by the layer thickness. Since the mechanical load is about the same for all the specimens, as the contact

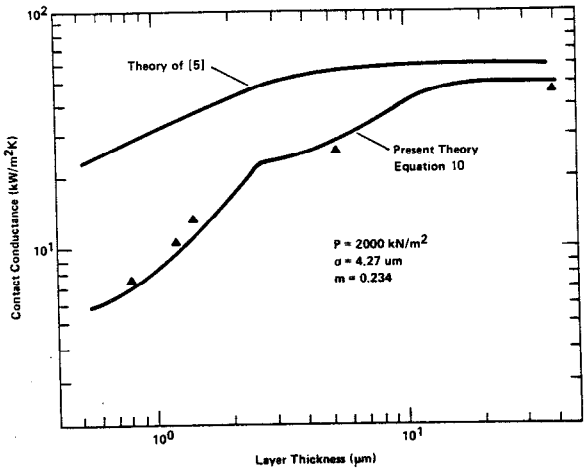

Fig. 6 Comparison of present theory and experimental data with theory of O'Callaghan et al. [5]

spot size decreases the number of contacts must increase in order to support the load. Further inspection of Table 2 reveals that the constriction parameter correction factor C and the resulting effective thermal conductivity k' are strongly dependent on the layer thickness, with only a slight dependence on the surface texture.

As mentioned previously, the only other model available against which the test results from this study can be compared is that of O'Callaghan et al. [5]. Figure .6 shows that the present theory predicts the test data from this work far better than the O'Callaghan et al. model.

Contact Correlation of Coated Specimen Test Data. The contact correlation for coated contacting surfaces is developed as follows. The bare contact conductance from Yovanovich's correlation [9] is substituted into equation (10) yielding

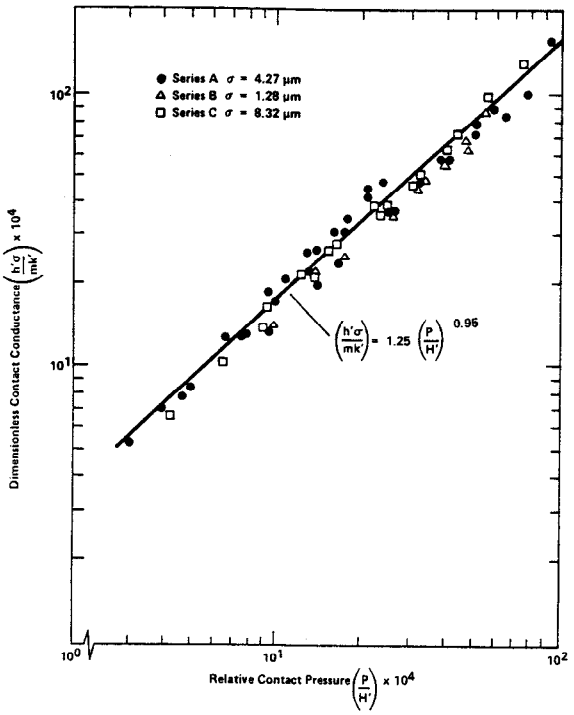

Fig. 7 Test results: dimensionless conductance versus relative pressure for coated contacting surfaces

$$h_j' = \left[1.25\left(\frac{m}{\sigma}\right)\left(\frac{2k_\alpha k_\beta}{k_\alpha + k_\beta}\right)\left(\frac{P}{H}\right)^{0.95}\right]\cdot \left(\frac{H}{H'}\right)^{0.93}\left(\frac{k_\alpha + k_\beta}{C_\alpha k_\beta + C_\beta k_\alpha}\right) \tag{22}$$

which reduces to

$$h_j' = 1.25\left(\frac{m}{\sigma}\right)\left(\frac{P}{H'}\right)^{0.95}\left(\frac{H'}{H}\right)^{0.02} k' \tag{23}$$

Now $(H'/H)^{0.02}$ is set equal to unity, essentially neglecting this term on the basis that the error introduced will be minimal. Equation (23) then simplifies to

$$\frac{h_j'\sigma}{mk'} = 1.25\left(\frac{P}{H'}\right)^{0.95} \tag{24}$$

Equation (24) for coated contacts is identical to the correlation for bare contacts given in [9], except that an effective thermal conductivity and an effective microhardness have replaced the usual values used for a bare joint.

Figure 7 shows that all coated test data correlate very well using equation (24). The overall RMS error for all coated data points is ±12.6 percent. In other words, using an effective microhardness and an effective thermal conductivity, the coated test data were correlated by [9] which had previously been used only for bare contacts. The implication is that a coated joint can be reduced to an equivalent bare joint by employing an effective microhardness and an effective thermal conductivity.

Conclusions

Based on this research, the major conclusions reached are: The thermomechanical model developed herein predicts the thermal contact conductance of the silver-coated contacting surfaces tested quite well; that a coated joint can be reduced to an equivalent bare joint by using the concepts of effective microhardness and effective thermal conductivity; and this then enables coated test data to be correlated by means of a correlation [9] developed for bare joints.

It is further concluded that a silver layer can enhance the thermal contact conductance of nominally flat, rough, contacting nickel specimens by as much as an order of magnitude; and that for a given layer thickness, the smoother the bare contacting surface the greater the enhancement will be.

Finally, is should be noted that this research applies only to nominally flat surfaces and is not applicable to nonflat contacting surfaces. In addition, a limited material set was tested, and although we believe the methodology presented is applicable to other materials, this has not been demonstrated.

Acknowledgments

M. M. Yovanovich acknowledges the partial support of the National Science and Engineering Research Council of Canada, under operating grant A7445.

References

1 Fry, E. M., "Measurements of Contact Coefficients of Thermal Conductance," AIAA 65-662, AIAA Thermophysics Specialists Conference, Monterey, CA, Sept. 1965.

2 Fried, E., and Kelley, M. J., "Thermal Conductance of Metallic Contacts in a Vacuum," AIAA-65-661, AIAA Thermophysics Specialists Conference, Monterey, CA, Sept. 1965.

3 Cunnington, G. R., Jr., "Thermal Conductance of Filled Aluminum and Magnesium Joints in Vacuum Environment," ASME Paper No. 64-WA/HT-40, 1964.

4 Molgaard, J., and Smelter, W. W., "The Thermal Contact Resistance at Gold Foil Surfaces," *Int. J. Heat Mass Transfer*, Vol. 13, 1970, pp. 1153–1162.

5 O'Callaghan, P. W., Snaith, B., Probert, S. D., and Al-Astrabadi, F. R., "Prediction of Interfacial Filler Thickness for Minimum Thermal Contact Resistance," *AIAA Journal*, Vol. 21, No. 9, Sept. 1983, pp. 1325–1330.

6 Mal'kov, V. A., and Dobashin, P. A., "The Effect of Soft-Metal Coatings and Linings on Contact Thermal Resistance," *Inzhenerno-Fizicheskii Zhurnal*, Vol. 17, No. 5, Nov. 1969, pp. 871–879.

7 Kharitonov, V. V., Kozhosev, L. S., and Tyurin, Y. A., "Effect of Thermal Conductivity of Surface Layer on Contact Thermal Resistance," *Atomnaya Energiya*, Vol. 36, No. 4, Apr. 1974, pp. 308–310.

8 Yovanovich, M. M., Tien, C. H., and Schneider, G. E., "General Solution of Constriction Resistance Within a Compound Disk," Presented as Paper 79-1178 at the AIAA 17th Aerospace Sciences Meeting, New Orleans, LA, Jan. 1979.

9 Yovanovich, M. M., "Thermal Contact Correlations," in: *AIAA Progress in Astronautics and Aeronautics: Spacecraft Radiative Transfer and Temperature Control*, ed. T. E. Horton, New York, 1982.

10 Chen, W. T., and Engle, P. A., "Impact and Contact Stress Analysis in Multilayer Systems," *Int. J. Solid Structures*, Vol. 8, 1972, pp. 1257–1281.

11 Yovanovich, M. M., Burde, S. S., and Thompson, J. C., "Thermal Constriction Resistance of Arbitrary Planar Contacts With Constant Flux," in: *AIAA Progress in Astronautics and Aeronautics, Thermophysics of Spacecraft and Outer Entry Probes*, ed. A. M. Smith, Vol. 56, New York, 1977, pp. 127–139.

12 Cecco, V. S., and Yovanovich, M. M., "Electrical Measurements of Joint Resistance at Perfect Contact Interfaces: Application to Joint Conductance," AIAA-72-19, AIAA 10th Aerospace Sciences Meeting, San Diego, CA, Jan. 1972.

13 Roess, L. C., "Theory of Spreading Conductance," Appendix to N. D. Weills, and E. A. Ryder, "Thermal Resistance Measurements on Joints Formed Between Stationary Metal Surfaces," presented at Semi-Annual ASME Heat Transfer Division meeting, Milwaukee, WI, 1948.

14 Mikic, B. B., and Rohsenow, W. M., "Thermal Contact Resistance," M.I.T. Heat Transfer Lab Report 4542-42, Sept. 1966.

15 Yovanovich, M. M., "General Expression for Circular Constriction Resistances for Arbitrary Heat Flux Distribution," in: *AIAA Progress in Astronautics and Aeronautics: Radiative Transfer and Thermal Control*, ed. A. M. Smith, Vol. 49, New York, 1976, pp. 301–308.

16 Cooper, M. G., Mikic, B. B., and Yovanovich, M. M., "Thermal Contact Conductance," *Int. J. Heat Mass Transfer*, Vol. 12, 1969, pp. 274–300.

17 Antonetti, V. W., "On the Use of Metallic Coatings to Enhance Thermal Contact Conductance," Ph.D. thesis, University of Waterloo, 1983.

18 Mulhearn, T. O., "The Deformation of Metals by Vickers-Type Pyramidal Indenters," *J. Mech. Phys. Solids*, Vol. 7, 1959, pp. 85–96.

19 Yovanovich M. M., Hegazy, A. H., and DeVaal, J., "Surface Hardness Distribution Effects Upon Contact Gap and Joint Conductances," AIAA-82-0887, Joint AIAA/ASME Heat Transfer, Fluids and Thermophysics Conference, St. Louis, MO, June 1982.

20 Yovanovich, M. M., Hegazy, A., and Antonetti, V. W., "Experimental Verification of Contact Conductance Models Based Upon Distributed Surface Micro-Hardness," AIAA-83-0532, AIAA 21st Aerospace Sciences Meeting, Reno, NV, Jan. 1983.

21 Antonetti, V. W., and Yovanovich, M. M., "Using Metallic Coatings to Enhance Thermal Contact Conductance of Electronic Packages," presented at 1983 ASME Winter Annual Meeting, Heat Transfer in Electronic Equipment Session, Boston, MA, November 1983.

22 Tamai, T., and Tsuchiya, T., "Direct Observation for the Effect Electric Current on Contact Interface," *Proceedings of the Ninth International Conference on Electric Contacts*, Chicago, IL, 1978, pp. 469–474.